

An energy-duration procedure for rapid determination of earthquake magnitude and tsunamigenic potential

Anthony Lomax¹, Alberto Michelini² and Alessio Piatanesi²

¹*A Lomax Scientific, Mouans-Sartoux, France. E-mail: anthony@alomax.net*

²*Istituto Nazionale di Geofisica e Vulcanologia (INGV), Roma, Italy*

Accepted date. Received date; in original form 6 October 2006

Abbreviated title: Energy-duration magnitude

Corresponding author: Anthony Lomax, +33 (0)493752502, alomax@free.fr

Summary

We introduce a rapid and robust, energy-duration procedure, based on the Haskell, extended-source model, to obtain an earthquake moment and a moment magnitude, M_{ED} . Using seismograms at teleseismic distances (30° - 90°), this procedure combines radiated seismic energy measures on the P to S interval of broadband signals and source duration measures on high-frequency, P -wave signals. The M_{ED} energy-duration magnitude is scaled to correspond to the Global Centroid-Moment Tensor (CMT) moment-magnitude, M_w^{CMT} , and can be calculated within about 20 minutes or less after OT. The measured energy and duration values also provide the energy-to-moment ratio, Θ , used for identification of tsunami earthquakes. The M_{ED} magnitudes for a set of recent, large earthquakes match closely M_w^{CMT} , even for the largest, great earthquakes; these results imply that the M_{ED} measure is accurate and does not saturate. After the 26 December 2004, Sumatra-Andaman mega-thrust earthquake, magnitude estimates available within 1 hour of OT ranged from $M = 8.0$ to $M = 8.5$, the CMT magnitude, available about 3 hours after OT, was $M_w^{CMT} = 9.0$, and, several months after the event, $M_w = 9.1$ - 9.3 was obtained from analysis of the Earth's normal modes. The energy-duration magnitude for this event is $M_{ED} = 9.2$, a measure that is potentially available within 20 minutes after OT. After the 17 July 2006, Java earthquake, the magnitude was evaluated at $M = 7.2$ at 17 minutes after OT, the CMT magnitude, available about 1 hour after OT, was $M_w^{CMT} = 7.7$; the energy-duration results for this event give $M_{ED} = 7.8$, with a very long source duration of about 160 sec, and a very low Θ value, indicating a possible tsunami earthquake.

Key words: seismic moment, Richter magnitude, earthquakes, tsunami, seismograms, waveform analysis

Introduction

The 26 December 2004, M9 ($M_w^{CMT}=9.0$) Sumatra-Andaman mega-thrust earthquake caused a tsunami that devastated coasts around the Eastern Indian Ocean within 3 hours; the 17 July 2006, $M_w^{CMT}=7.7$ Java earthquake caused an unexpectedly large and destructive tsunami. For both events the magnitude and other information available within the first hour after the event origin time (OT) severely underestimated the event size and tsunamigenic potential (PTWC, 2004ab; Kerr, 2005; PTWC, 2006ab).

Tsunami hazard warning and emergency response for future large earthquakes would benefit greatly if

accurate knowledge of the earthquake size and tsunamigenic potential were available rapidly, within 30 minutes or less after OT. Currently, the earliest, accurate estimates of the size of major and great earthquakes come from moment tensor determinations, including the authoritative, Global Centroid-Moment Tensor (CMT) (Dziewonski et al., 1981; Ekström, 1994) and related procedures (e.g., Kawakatsu, 1995). These estimates are based on long-period, seismic S and surface-wave waveform recordings, but these recordings, and thus the event size estimates, are typically not available until an hour or more after OT.

There are a number of procedures for rapid analysis of large earthquakes currently in use at earthquake and tsunami monitoring centers. The NEIC Fast Moment Tensor procedure (NEIC, 2004) produces an estimate of the seismic moment tensor for earthquakes of magnitude of 5.5 or greater within the order of 30 min after OT through automated processing and inversion of body-wave waveforms. The NEIC Fast Moment Tensor magnitudes for the 2004 Sumatra-Andaman and 2006 Java, earthquakes are $M_w=8.2$ and $M_w=7.2$, respectively.

The Pacific Tsunami Warning Center (PTWC) uses the M_{wp} moment magnitude algorithm, and the PTWC and the Papeete, Tahiti, tsunami center (Centre Polynésien de Prévention des Tsunamis) use the mantle magnitude, M_m , to rapidly estimate the size of large earthquake (e.g., Weinstein and Okal, 2005; Weinstein *et al.*, 2005; Hirshorn, 2006). The M_{wp} moment magnitude algorithm (Tsuboi *et al.*, 1995; Tsuboi *et al.*, 1999; Tsuboi, 2000) considers broadband, P displacement seismograms as approximate far-field, source-time functions. These displacement seismograms are integrated and corrected approximately for geometrical spreading and an average P wave radiation pattern to obtain scalar moments at each station. Application of the standard moment magnitude formula and averaging over stations produces a moment magnitude, M_{wp} , for the event. Because the M_{wp} calculation used only the P wave portion of a seismogram, this magnitude estimate is potentially available only a few minutes after the P waves are recorded at teleseismic distances, *i.e.* about 10 min after OT at a great-circle distance (GCD) of 30° , and about 18 min after OT at 90° GCD. The M_{wp} magnitudes for the 2004 Sumatra-Andaman and 2006 Java, earthquakes are $M_w = 8.0$ (PTWC, 2004a) and $M_{wp} = 7.2$ (PTWC, 2006a), respectively, much less than the corresponding CMT magnitudes. In contrast, for the 28 March, 2005, Northern Sumatra earthquake, $M_{wp} = 8.5$ was obtained only 19 min after OT (Weinstein *et al.*, 2005), a close match to the $M_w^{CMT} = 8.6$.

The mantle magnitude M_m (Okal and Talandier, 1989; Newman and Okal, 1998; Weinstein and Okal, 2005) is based on measurements of the spectral amplitude of mantle Rayleigh waves at variable periods (between 50 and 300 sec for large events). These amplitudes, combined with approximate corrections for geometrical spreading and for the excitation of Rayleigh waves at the source, give the M_m estimate and a corresponding moment. The M_m magnitude is potentially available within minutes after the first Rayleigh wave passage, *i.e.* about 20 min after OT at 30° GCD, and about 50 min after OT at 90° GCD. A standard M_m magnitude procedure underestimated the size of the 2004 Sumatra-Andaman earthquake (Weinstein *et al.*, 2005), but analysis of waves at increased periods (450 sec or more) may improve the M_m estimates for very large events (Weinstein and Okal, 2005; UNESCO, 2005).

Seismic P waves are the earliest signal to arrive at seismic recording stations. At teleseismic distances, the arrival times of the initial P -wave are used routinely to locate the earthquake hypocentre, within about 15 minutes after OT. Comprehensive information about the event size and source character is contained in the initial P -waves and in the following P -wave train. For example, the body wave magnitude (e.g., Gutenberg, 1945), m_b , is calculated from the amplitude and period of the first P -wave pulses. Boatwright and Choy (1986) show that the total radiated seismic energy can be estimated from the the P -waves alone. Recently, Menke and Levin (2005) proposed that the ratio of long-period, P -wave displacement amplitudes between an target event and a nearby reference event of know size can rapidly provide the magnitude of the target event. Lomax (2005) showed for very large earthquakes that the location of the end of rupture, and thus an estimate of the event size, could

be rapidly determined from measures of the P -wave duration on high-frequency records. Lomax and Michelini (2005) noted that the ratio of the high-frequency, P -wave durations from the 2004 Sumatra-Andaman and the 2005 Northern Sumatra earthquakes match the ratio of the CMT moment values for the two events, and suggested that the high-frequency, P -wave duration could be used for rapid magnitude estimation for individual events.

Here we introduce a rapid and robust, energy-duration procedure to obtain an earthquake moment and a moment magnitude, M_{ED} , from P -wave recordings from global seismic stations at 30° to 90° distance from an event. At many earthquake and tsunami monitoring centers, these recordings are currently available within 20 to 30 minutes after OT. The methodology combines a radiated seismic energy measured within the P to S interval on broadband records, and a source duration measured on high-frequency, P -wave records. The measured energy and duration values also provide the energy-to-moment ratio Θ (e.g., Newman, and Okal, 1998; Weinstein and Okal, 2005) for identification of tsunami earthquakes; these earthquakes are characterized by a deficiency in moment release at high frequencies (Kanamori, 1972; Polet and Kanamori, 2000; Satake, 2002), and a correspondingly low Θ value. The M_{ED} magnitude and the Θ ratio, combined with knowledge of the tectonics of the hypocentre zone, can aid in rapid assessment of tsunami hazard and damage distribution after large earthquakes. We apply our energy-duration methodology to a number of recent, large earthquakes with diverse source types.

Theoretical motivation

Haskell (1964) proposed a kinematic, double-couple, line-source fault model with scalar moment M_0 and a trapezoidal, far-field pulse in displacement with total duration T_0 and rise and fall times xT_0 . The factor x varies from $x = 0$ for a box-car, far-field pulse shape to $x = 0.5$ for a triangular pulse. With this model, and neglecting directivity, Vassiliou and Kanamori (1982) show that the radiated seismic energy, E , can be expressed as,

$$E = \left[\frac{1}{15\pi\rho\alpha^5} + \frac{1}{10\pi\rho\beta^5} \right] \frac{2}{x(1-x)^2} \frac{M_0^2}{T_0^3}, \quad (1)$$

where ρ , α and β are the density, and P and S wave speeds, respectively, at the source. Solving for M_0 we find, for a given rise-time factor, x , an *energy-duration* moment estimate,

$$M_0^{ED} = K x^{1/2} (1-x) E^{1/2} T_0^{3/2}, \quad (2)$$

where K depends on ρ , α and β at the source. This compact expression suggests that the scalar moment, M_0^{ED} , for an earthquake can be obtained from estimates of the radiated energy, E , and the source duration, T_0 . This energy-duration moment is proportional to the square-root of E and the cube of the square-root of T_0 , thus the accuracy of the moment estimate depends strongly on the accuracy of the source duration measure and, to a lesser degree, depends on the accuracy of the energy estimate.

Application to recent large earthquakes

We develop a rapid, energy-duration methodology based on Eq. 2 to determine moments and magnitudes, and the energy-to-moment ratio Θ . We apply this procedure to a set of recent earthquakes with a large range of magnitudes ($M_w^{CMT} = 6.6-9.0$) and diverse source types (Fig. 1; Table 1). For each event, we obtain from the IRIS Data Management Center a set of broadband vertical (BHZ) component recordings at stations from 30° to 90° GCD from the event. Typically we use about 20 to 50 records, selecting records well distributed in distance for events which have more than 50 available records; we assume that records are well distributed in azimuth since we ignore directivity effects. We exclude from the analysis poor quality seismograms that are noisy, clipped,

truncated, or otherwise corrupted. Such data sets, along with the corresponding hypocentre location and predicted P and S travel times to each recording station are available at many real-time monitoring agencies within 30 minutes or less after a large earthquake.

The source parameters and energy-duration results for the studies events are listed in Table 1. We classify the source types in Table 1 as follows: I - interplate thrust earthquakes (*e.g.*, events on the interface between a subducting slab and the overriding plate); T - tsunami earthquakes; P - intraplate earthquakes (*e.g.*, normal faulting events within a subducting slab); W - downdip subduction zone earthquakes ($\sim 50 \leq \text{depth} \leq 150$ km); D - deep subduction zone earthquakes (depth ≥ 150 km); S - strike-slip crustal earthquakes; R - reverse faulting crustal earthquakes; N - normal faulting crustal earthquakes.

Radiated seismic energy estimates

An estimate of the radiated seismic energy, E , for a point, double-couple source using a P -wave seismogram (*i.e.* the P to S interval on a vertical component record) is given by (*e.g.*, Boatwright and Choy, 1986; Newman, and Okal, 1998; Boatwright et al., 2002),

$$E = (1+q) 4\pi r^2 \frac{\langle F^P \rangle^2}{(F^{SP})^2} \rho \alpha \int v^2(t) dt, \quad (3)$$

where $v(t)$ is a ground-velocity seismogram, r is the source-station distance, and ρ and α are the density and P wave speed, respectively, at the station. $\langle F^P \rangle^2 = 4/15$ is the mean square radiation coefficient for P waves, and F^{SP} is a generalized radiation pattern coefficient for the P wave group (P , pP and sP). The factor $(1+q)$, $q=15.6$, compensates for the missing S energy. The term $4\pi r^2$ arises from the approximation that the energy estimate at a station represents the average energy density on a sphere of radius r , with simple, $1/r$ geometrical spreading.

The ground motion $v^2(t)$ must be corrected for the free-surface amplification at the station site, which introduces a factor of $1/4$, and for attenuation. The attenuation correction is often made in the frequency domain since attenuation varies with frequency. For simplicity, because of the wide range of attenuation relations proposed in the literature, and because we are ultimately interested in an algorithm that can be applied in real-time to produce time-evolving estimates of event size, we use here a constant, frequency-independent correction factor for attenuation. Taking a t^* (*e.g.*, Shearer, 1999; Lay, 2002) value of $t^*=0.8$, representative of the average t^* at period around 1-10 sec at $GCD = 60^\circ$ (Choy and Boatwright, 1995), we arrive at an energy correction factor for attenuation of about $\exp(-\pi f t^*) \approx 12$, using $f = 1$ Hz.

For rapid event analysis, we must also determine the factor F^{SP} in the absence of knowledge of the source parameters. For observations at teleseismic distances, following Newman and Okal (1998), we use a constant value $F^{SP}=1$ for the generalized radiation coefficient which is appropriate for dip-slip faulting but too high by about a factor of 4 for strike-slip faulting (Boatwright and Choy, 1986; Choy and Boatwright, 1995).

Combining all the above factors, we have,

$$E = 53 \pi r^2 \rho \alpha \int v^2(t) dt. \quad (4)$$

Substituting $\rho=2.6\text{g/cm}^3$, $\alpha=5\text{km/s}$ (representative values for the upper crust, where the stations are sited) and assuming $v(t)$ is ground velocity in units of m/s, we arrive at a station energy,

$$E = 2.2 \times 10^{15} r^2 \int v^2(t) dt, \quad (5)$$

where r has units of km and E units of N-m. In addition, if we find that the source duration, T_0 , is greater than the S - P interval, t_{S-P} , it is necessary to multiply the station energy by a factor T_0 / t_{S-P} .

Energy determination procedure and results

We estimate the radiated seismic energy E for each event using vertical-component seismograms and the following procedure (Fig. 2): 1) Remove the instrument response to convert each seismogram to ground-velocity in m/sec. 2) Cut each seismogram from 10 seconds before the P arrival to 10 seconds before the S arrival to obtain P -wave seismograms. 3) Apply Eq. 5 to each P wave seismograms to obtain station energy values. 4) Multiply the station energy value by a factor T_0 / t_{S-P} if $T_0 > t_{S-P}$. 5) Calculate an average E and associated standard deviation for each event by taking the geometric mean (the arithmetic mean of the logarithms) and geometric standard deviation of the station energy values. We use the geometric mean and standard deviation since E must be positive and thus is best represented by a log-normal distribution.

Table 1 and Fig. 3 show our radiated seismic energy values, E , for the studied events. Because we use recordings only from stations at $GCD \geq 30^\circ$, it is necessary to multiply by the station energy factor T_0 / t_{S-P} only for a few of the closest stations for the largest event (2004.12.26 Sumatra-Andaman); the inclusion of this factor does not change appreciably the energy-duration results for this event.

Table 1 and Fig. 3 show that our values, E , for radiated energy, excluding strike-slip events, agree well with the radiated energy values, E_S , determined by the NEIC using the procedure of Boatwright and Choy (1986). Our E values are less than those of Venkataraman and Kanamori (2004; their mean and median values) and of Newman, and Okal (1998; their E^E and E^T values) for the corresponding events, perhaps because these authors use larger ρ and α values than those we use in our Eq. 4. Our E estimate of 1.4×10^{17} N-m for the 2004 Sumatra-Andaman event (2004.12.26 Sumatra-Andaman) is the same as the E_S value determined by NEIC, less than the value of 1.1×10^{18} N-m of Lay et al. (2005), and compatible with the range of values of 1.38×10^{17} - 3.0×10^{17} N-m determined by Kanamori (2006) using several methods

For all the studied strike-slip earthquakes, however, we obtain E values that are less than those of NEIC by a factor of about 10, on average (Table 1, Fig. 3). All of these events have steeply dipping nodal axes close to which teleseismic P rays depart from the source. Thus the discrepancy in radiated energy estimates is likely due to the use in the NEIC calculation of a generalized radiation pattern coefficient $F^{SP} \sim 0.25$ for strike-slip events, which would introduce a correction factor to E of $1/0.25^2 \approx 16$ (e.g., Boatwright and Choy, 1986; Newman, and Okal, 1998). In our energy calculation we ignored focal mechanism variations and thus may underestimate the radiated energy for strike-slip events.

In the following, to allow meaningful comparison of our results with CMT values, we increase our radiated seismic energy values, E , by a factor of 10 for strike slip events to approximately account for this energy underestimate (Table 1, E corrected). This factor increases the M_{ED} magnitude estimate by around 0.2-0.3 magnitude units relative to the value that would be obtained with the underestimated E . We also note that, for some of the strike-slip events, using the underestimated E values gives large, negative values of energy-to-moment ratio Θ , similar to the values indicative of a tsunami earthquake. Thus, as with all rapid analysis methodologies based on body-wave signals, knowledge of the source location, its tectonic setting and likely focal mechanism is needed to obtain the most accurate magnitude and to distinguish low Θ values corresponding to strike-slip events and those indicative of tsunami earthquakes.

Source duration estimates

In this study, we estimate the source duration, T_0 , from P -wave seismograms using high-frequency analysis methods from strong motion source studies (e.g., Gusev and Pavlov, 1991; Cocco and Boatwright, 1993; Zeng *et al.*, 1993). This estimate relies on three basic assumptions: 1) at a recording station, P -waves radiated from the rupture contain higher frequencies than other wave types; 2) this signal can be isolated on the seismograms; 3) a meaningful time for the end of this signal can be determined. Observations and experience support the first two assumptions. For example, stacks of short period (< 2 s), vertical-component seismograms from large numbers of earthquakes (Shearer, 1999, his Fig. 4.18) shows that the direct P wave signal is the most energetic wave type to about 110°

GCD. For example, for the 2004 Sumatra-Andaman event, short period signals (~ 1 Hz) from a large aftershock (M7.2, 2004 Dec 26, 04:21 UT) show little or no signal from later phases (e.g., PcP , PP , S) relative to the amplitude of the initial, direct P signal (Fig. 4). However, in some cases the direct S wave or other phases can have high-frequency content which overlaps the direct P signal. The third assumption poses difficulties since the isolated, high-frequency, P -wave signal usually has an exponentially decaying coda caused by wave scattering that does not present a unique ending time for this signal.

We thus obtain the source duration, T_0 , for each event using vertical-component seismograms and the following procedure (Fig. 5), based on that of Lomax (2005): 1) Convert the seismograms from each station to high-frequency records using a narrow-band, Gaussian filter of the form $e^{-\alpha(|f-f_{cent}|/f)^2}$, where f is frequency, f_{cent} the filter center frequency, and α sets the filter width (here we use $f_{cent} = 1.0$ Hz and $\alpha = 10.0$). 2) Convert each high-frequency seismogram to pseudo kinetic-energy density by squaring each of the velocity values. 3) Smooth each velocity-squared time-series with a 10 sec wide, triangle function and normalize to form an envelope function. 4) Stack the station envelope functions aligned on their P arrival times to form a summary envelope function for the event. 5) Measure a source end time, T_{end} , defined as the mean of the times where the event envelope function last drops below 50% and below 33% of its peak value. 6) Calculate the source duration T_0 from the difference between T_{end} and the stack alignment P time.

The choice of 50% and 33% of the envelope peak value to measure source end times T_{end} follows from examination of the shape of the summary envelope functions used in this study (e.g., Fig. 5). In general, the 33% peak value gives better results for the larger events (e.g., Table 1, 2004.12.26 Sumatra-Andaman) and the 50% peak value better results for the smallest events, in comparison to expected values and other estimates of source duration. This difference is due to the longer length of the exponentially decaying P coda relative to the source duration for smaller events than for larger events (c.f., the two traces in Fig. 4).

A comparison between our estimates of source duration, T_0 , and the CMT duration (i.e., 2 x the CMT half-duration; Table 1) shows that our T_0 values are on average about twice the CMT duration. However, our mean value of $T_0 = 420$ s and 33% envelope peak value of $T_0 = 473$ s for 2004.12.26 Sumatra-Andaman are closer than the CMT duration of 190s to the inferred value for the full, co-seismic rupture of about 450-600s for this event (e.g. Lomax, 2005; Ammon, *et al.*, 2005). Thus for the larger events, at least, our T_0 values may be good estimates of the duration of co-seismic faulting. For the smallest events studied ($M_w < \sim 7$), the expected duration of faulting is less than the typical P coda length on the high-frequency seismograms (e.g., Fig. 4, lower trace) and of the same order as the width of the triangular smoothing function used to generate the envelope functions, thus our T_0 values are subject to relatively large uncertainty. In particular, we get T_0 values which are larger than CMT duration by a factor of 3 or more for three strike-slip events with $M_w \sim 7$ (2000.10.06 Honshu; 2003.09.27 Siberia, 2003.12.26 S Iran).

Energy-duration moment and magnitude calculation

From the obtained values of the radiated seismic energy, E , and the source duration, T_0 , we calculate an energy-duration estimate of the seismic moment, M_0^{ED} , using Eq. 2. Unless otherwise stated, we use for each event the ρ , α and β values for the PREM model (Dziewonski and Anderson, 1981) at the CMT centroid depth for the event. Using these values we can compare directly our results to the corresponding M_0^{CMT} and M_w^{CMT} estimates. For the same reason, as discussed earlier, we increase the radiated seismic energy values, E , by a factor of 10 for strike-slip events to approximately account for our energy underestimate for these events. For rapid, real-time analysis, if a reliable source depth is not available, the use of average material properties for the the lower crust and upper mantle (e.g.,

following Newman and Okal (1998), $\rho = 3 \text{ g/cm}^3$, $\alpha = 7 \text{ km/sec}$ and $\beta = 4 \text{ km / sec}$) changes the final energy-duration moment magnitude estimates by about 0.1 magnitude unit or less for events shallower than about 200km, while the use of uncorrected E values decreases the magnitude estimate by around 0.2-0.3 magnitude units for strike-slip events.

We calibrate the unknown rise-time factor, x , in Eq. 2. through regression of our M_0^{ED} values for each event against the corresponding CMT moment values, M_0^{CMT} , so that the mean of $\log_{10}(M_0^{ED}/M_0^{CMT}) \rightarrow 0$. For this regression we exclude all strike-slip events because of the instabilities in their energy and duration estimates, however, if we include these events the calibration changes little, since $M_0^{ED} \propto E^{1/2}$ (c.f. Eq. 2). We also exclude the 26 December 2004, M9 Sumatra-Andaman and 17 July 2006, $M_w^{CMT} = 7.7$ Java earthquakes to allow an unbiased assessment of the energy-duration results for these events. The regression gives a rise-time $xT_0 \approx 0.005T_0$, which implies a near box-car shape, on average, for the far-field pulse for the large events studied here. This value for x is also much smaller than the value of $x \approx 0.2$ assumed by Vassiliou and Kanamori (1982), which suggests that their energy estimates could be too small by a factor of as much as 25. Our regression result, however, is strongly dependent on several poorly known or approximate factors used in Eq. 3 to estimate radiated seismic energy, E , and on any error or bias in our estimates of the source duration, T_0 . Vassiliou and Kanamori (1982) also require estimates of T_0 , which may not be compatible with our estimates. Further work is therefore needed to fully understand the implications of the value of x we obtain here to the estimation of radiated energy and to rupture physics.

We calculate an energy-duration magnitude, M_{ED} , through application of the standard moment to moment magnitude relation (Kanamori, 1977; Kanamori, 1978; Hanks and Kanamori, 1979),

$$M_{ED} = (\log_{10} M_0^{ED} - 9.1) / 1.5, \quad (6)$$

where M_0^{ED} has units of N-m. We estimate an uncertainty for M_0^{ED} and M_{ED} for each event by re-evaluating Eqs 2 and 5 using the geometric mean of E minus (plus) the geometric standard deviation of E and the 50% (33%) peak duration values, T_0 , to obtain a lower (upper) bound on M_0^{ED} and M_{ED} .

Comparison of M_{ED} and M_w^{CMT}

Our ensemble of seismic moment estimates, M_0^{ED} , and energy-duration magnitudes, M_{ED} , necessarily correspond roughly to the M_0^{CMT} and M_w values (Table 1) since we calibrated M_0^{ED} against M_0^{CMT} . More important and striking is the small scatter and low standard-deviation ($\sigma=0.16$ magnitude units) of M_{ED} relative to M_w^{CMT} , and the very good match between M_{ED} and M_w^{CMT} for individual events at all magnitudes (Table 1, Fig. 6), including great earthquakes and the 2004, M9 Sumatra-Andaman earthquake (2004.12.26 Sumatra-Andaman; $M_w^{CMT} = 9.0$, $M_{ED} = 9.2$). These results indicate that a rapidly determined, M_{ED} value should provide a robust and accurate estimate of the moment magnitude of future, large earthquakes, including the largest, great events.

Fig. 6 shows increased uncertainty in M_{ED} and increased differences between M_{ED} and M_w^{CMT} for the smallest events ($M_w < \sim 7$). These increases are to be expected since there is a relatively large uncertainty in our T_0 estimates for smaller events (recall that M_{ED} is a function of $T_0^{3/2}$, c.f. Eq. (2)) and because these events have a wide variety of source types, including strike-slip events, for which our radiated energy estimates can be unstable.

The M_{ED} and M_w^{CMT} magnitude measures are based on different analysis procedures emphasizing different aspects of the radiated earthquake waves. M_0^{ED} and M_{ED} are calculated from a direct, broadband measure of the radiated seismic energy, E , and a direct measure of the source duration, T_0 , which provides the equivalent of very long-period information. In contrast, M_0^{CMT} and M_w^{CMT} are determined through inversion of long-period, displacement seismograms. Physically, the M_{ED}

measure emphasizes shaking intensity and source duration, while the M_w^{CMT} measure seeks to quantify a static change in elastic strain in the volume around the source by isolating the longest periods in the signal. Thus the two magnitudes M_{ED} and M_w can be expected to respond differently to events with different source mechanisms, far-field pulse shapes, or tectonic settings. Similarly, as with other rapid analysis methodologies based on body-wave signals, information on the location, tectonic setting and likely focal mechanism of an event are required to obtain the best match to CMT estimates of moment and magnitude.

Despite these differences, M_{ED} and M_w^{CMT} agree within less than 0.25 magnitude units for most of the events examined here (Table 1). The four events for which $M_{ED} \geq M_w^{CMT} + 0.25$ are all crustal, strike-slip events (2000.10.06 W Honshu, 2003.09.27 Siberia, 2003.12.26 S Iran, 2005.07.24 Nicobar), and strike-slip events were excluded from our calibration of M_{ED} against M_w^{CMT} . For all of these events the NEIC energy magnitude, M_e , is larger than the M_w^{CMT} , indicating that their radiated seismic energy may have been anomalously large. However, these four events are also some of the smallest events we analyze and thus subject to large, relative error in the duration measure, T_0 , with an overestimation of T_0 most likely.

There are no events for which $M_{ED} \leq M_w^{CMT} - 0.25$. However, for a great, interplate earthquake (2005.03.28 Northern Sumatra), $M_{ED} = 8.4$ is 0.2 magnitude units less than $M_w^{CMT} = 8.6$. This event produced an anomalously small tsunami, possibly due to concentration of slip in the down-dip part of the rupture zone, with much of the vertical displacement field occurring around islands in shallow water or on land (Geist *et al.*, 2006). If the length and width of rupture for this event were of similar size, then the Haskell, extended fault model used in deriving in Eq. 2 is not ideal for this event. Also, if the far-field pulse shape for this event is closer to a triangle than to a box-car, relative to the other studied events, then our M_0^{ED} and M_{ED} values may be underestimated, since a triangular function implies a larger value of $x^{1/2}(1-x)$ in Eq. 2 than we use here.

Energy-to-moment ratio

From the obtained values of the radiated seismic energy, E , and our calculated seismic moment estimate, M_0^{ED} , we can determine the energy-to-moment ratio parameter, Θ , (*e.g.*, Newman, and Okal, 1998; Weinstein and Okal, 2005) for identification of tsunami earthquakes,

$$\Theta = \log_{10} \frac{E}{M_0^{ED}}. \quad (7)$$

For most earthquakes, this parameter is expected to have a value of $\Theta \approx -4.9$, but Θ values as low as -5.9 to -6.3 are found for tsunami earthquakes (Weinstein and Okal, 2005). Thus anomalously low values of a rapid estimate of Θ , combined with knowledge of an earthquake's location, size, tectonic setting and likely source type, can be an important indicator of a potential tsunami earthquake.

Our energy-to-moment ratio values, Θ , are close to the values of Newman and Okal (1998; their Θ^T values) for the corresponding events (Table 1). Fig. 7 shows $\log_{10} E$ vs. $\log_{10} M_0^{ED}$ and two lines of constant Θ : $\Theta = -4.9$, the expected value for all earthquakes, and $\Theta = -5.5$, below which indicates a possible tsunami earthquake (*e.g.*, Weinstein and Okal, 2005).

Discussion

The energy-duration analysis we have introduced in this paper, when applied to a set of recent, large earthquakes ($M_w^{CMT} = 6.6-9.0$), produces an energy-duration magnitude, M_{ED} , which matches well M_w^{CMT} for individual events at all magnitudes, including the largest great earthquakes (Table 1, Fig. 6). Thus the M_{ED} magnitude is accurate and apparently does not saturate for large events, as does, for example, the m_b body wave magnitude at around $m_b = 6$, and the M_s surface wave magnitude at about $M_s = 7.5$ (*e.g.* Utsu, 2002). These results indicate that the robust, energy-duration procedure and

magnitude, M_{ED} , can give rapid, accurate and useful quantification of size for future large and great earthquakes.

The robustness and accuracy of our energy-duration procedure can be attributed to the combined use of two quasi-independent measures, one of energy and the other of duration, which quantify different physical characteristics of an earthquake. In addition, the energy-duration procedure uses broadband and high-frequency signals, which typically have higher signal-to-noise levels and little instability relative to the long-period, narrow-band or integrated signals required by most other non-saturating methods for magnitude determination of major and great earthquakes.

Comparison with M_{wp}

The M_{wp} moment magnitude (Tsuboi *et al.*, 1995; Tsuboi *et al.*, 1999; Tsuboi, 2000) is calculated from integrated, vertical-component, displacement seismograms containing the P and pP waves. M_{wp} can be determined rapidly (about 10-20 min after OT at teleseismic distances) and is effectively a long period estimate. Because M_{wp} is currently in use for rapid earthquake size assessment (*e.g.* at the PTWC: Weinstein *et al.*, 2005; Hirshorn, 2006) and can be determined as fast or faster than M_{ED} , we examine here recalculated M_{wp} magnitudes for the studied events (Table 1, Fig. 8). In calculating these M_{wp} magnitudes, we follow strictly the procedure described by Tsuboi (2000) and Hirshorn (2006), including hand picking of amplitudes on the integrated displacement waveforms; we average readings from 2 to 29 stations, using 13 station on average, and obtain standard-deviation uncertainties for each event of about $\sigma=0.3$ magnitude units. We find that care must be taken when integrating the displacement seismograms and in reading the peak amplitudes to avoid errors due to long period noise and offsets in the waveforms (*c.f.* Tsuboi *et al.*, 1999).

Our Table 1 and Fig. 8, and the results of Tsuboi *et al.* (1999, their Fig. 2) and Hirshorn (2006), show that M_{wp} matches closely M_w^{CMT} up to $M_w^{CMT} \sim 7.5$, while above this magnitude M_{wp} tends to underestimate M_w^{CMT} . In particular, our M_{wp} estimates for the 2004.12.26 Sumatra-Andaman ($M_w^{CMT} = 9.0$, $M_{ED} = 9.2$), the 2005.03.28 Sumatra ($M_w^{CMT} = 8.6$, $M_{ED} = 8.4$), and the 2006.07.17 Java, tsunami earthquake ($M_w^{CMT} = 7.7$, $M_{ED} = 7.8$) events are $M_{wp} = 8.1$, 8.2 and 7.2, respectively. These M_{wp} values are consistent with the rapid, M_{wp} estimates of the PTWC (8.0, 8.5 and 7.2, respectively; PTWC, 2004a, 2006a; Weinstein *et al.*, 2005). Recently, Kanjo *et al.* (2006) have proposed a correction factor for M_{wp} to account for distance-dependent, apparent P -velocity. This correction increases M_{wp} to 8.5 for the 2004.12.26 Sumatra-Andaman event, and to 8.7 for the 2005.03.28 Sumatra event. However, all these results indicate that M_{wp} saturates above $M_w^{CMT} \sim 7.5$, and suggest that some of the largest, M_{wp} underestimates of M_w^{CMT} occur for tsunami earthquakes and tsunamigenic events (*e.g.* 1992.09.02 Nicaragua, 2001.06.23 Peru, 2004.12.26 Sumatra-Andaman, and 2006.07.17 Java). In contrast, we find a good match between M_{ED} and M_w^{CMT} for all events above $M_w^{CMT} \sim 7.0$, including great and tsunami earthquakes (Table 1, Fig. 6). Thus M_{wp} can provide rapid and accurate magnitude estimates for events smaller than $M_w^{CMT} \sim 7.5$, while M_{ED} , at teleseismic distances, may be an optimal method to provide rapid and accurate magnitude estimates for events larger than $M_w^{CMT} \sim 7.0$.

Energy-to-moment ratio Θ , Duration T_0 and tsunami earthquakes

The energy-to-moment ratio, Θ , is an important discriminant for potential tsunami earthquakes (*e.g.*, Newman, and Okal, 1998; Weinstein and Okal, 2005). Tsunami earthquakes are characterized by a deficiency in moment release at high frequencies (Kanamori, 1972; Polet and Kanamori, 2000; Satake, 2002), and a correspondingly low Θ value. Pelayo and Wiens (1992) studied several tsunami earthquakes and found double-couple mechanisms with long source durations for each of them; these earthquakes were shallow, occurring under accretionary prisms in Peru and the Kurile Islands. Pelayo and Wiens (1992) favored relatively slow rupture propagation along the basal decollement of the accretionary prism as the explanation for the slow nature of these earthquakes, rather than earthquake triggered slumping, which has been proposed as the source of many tsunami earthquakes. Kanamori and Kikuchi (1993) studied the 1992 Nicaragua earthquake, which caused a large and destructive

tsunami with a local amplitude of 10 m on the Nicaraguan coast, but which occurred in an area with no accretionary prism. The characteristics of this earthquake led Kanamori and Kikuchi (1993) to argue that there may be two types of tsunami earthquakes, those that arise from slow rupture, which they attribute to the effect of subducted sediments within the subduction interface (see also Polet and Kanamori, 2000), and those, such as the 1896 Sanriku and 1946 Unimak Islands earthquakes, which may involve large-scale, submarine slumping. The energy-to-moment ratio Θ is expected to be anomalously low for slow, tsunami earthquakes ($\Theta \leq -5.5$), but not necessarily anomalous for events that may trigger large-scale slumping.

Our energy-duration analysis finds very low values of Θ ($\Theta \leq -5.5$; Table 1; Fig. 7) for all four, known tsunami earthquakes we examine (1992.09.02 Nicaragua, 1994.06.02 Java, 1996.02.21 Peru, 2006.07.17 Java), for a tsunamigenic event (1998.07.17 Papua New Guinea) that is not thought to be a tsunami earthquake (Heinrich *et al.*, 2001; Okal, 2003), for the 2004 Sumatra-Andaman mega-thrust (2004.12.26), and for two interplate (2001.06.23 Peru and 2005.08.16 Honshu) and one intraplate events (2001.03.24 Honshu). As noted earlier, without the strike-slip energy correction most of the non-oceanic, crustal strike-slip events we examine (e.g. 1999.10.16 California, 2000.10.06 Honshu, 2003.09.27 Siberia, 2003.12.26 S_Iran) would also have $\Theta \leq -5.5$.

We also obtain the largest duration values, T_0 , relative to the CMT centroid durations for many of the events for which we find $\Theta \leq -5.5$ (Table 1). One of these events, 1998.07.17 Papua New Guinea, had a delayed main rupture (Kikuchi *et al.*, 1999), which could explain an anomalously long, high-frequency rupture duration relative to the calculated moment. Overall, however, this result support the idea that a low value of Θ for tsunami earthquakes is related to an anomalously long source duration due to a slow rupture velocity and large fault length relative to width, since Θ is proportional to $T_0^{-3/2}$ (*c.f.*, Eqs 2 and 7).

In practice, information on the location, tectonic setting and likely focal mechanism of an event will usually be available before the energy-duration analysis is completed; this information is required for all rapid analysis methodologies based on body-wave signals. Thus the tectonic nature of events with low values of Θ and large T_0 can be determined rapidly. Strike-slip and deeper events, which are not likely to be tsunamigenic, can be associated with low hazard, while large and shallow, interplate thrust events can be identified as possible tsunamigenic or tsunami earthquakes.

An additional impediment to rapid identification of tsunami and other, shallow, tsunamigenic earthquakes arises because to the true shear velocities and rigidities around the source may be much lower than the values in standard models such as PREM. In this case, the estimates of seismic moment by any procedure will be biased and there will be an ambiguity between moment and slip amplitude. This difficulty is ameliorated with the energy-duration procedure, since the duration, T_0 , and energy-to-moment ratio, Θ , are immediately available as robust, additional indicators for events that are shallow and have slow rupture, and thus which may be tsunamigenic.

Rapid application at near-teleseismic and closer distances

The energy-duration methodology can produce estimates of the magnitude, M_{ED} , and moment ratio, Θ , for a large earthquake within 25 min of OT if stations up to 90° GCD and the complete P to S body wave waveforms are used for analysis. However, it is likely that accurate results can be obtained more rapidly from observations at closer distances, for examples from 30° to 50° GCD. For the 17 July 2006, $M_w=7.7$ Java, earthquake, the energy-duration procedure applied to 11 P to S records from stations at 30° to 50° GCD (available within 17 min of OT), and using average, lower crust and upper mantle material properties at the source, produces $M_{ED}=7.9$ and $\Theta = -6.0$, nearly the same as the values obtained above using about 50 stations at 30° to 90° GCD and the material properties at the CMT centroid depth. In addition, the energy-duration analysis can be terminated before the S arrival time for records where the energy integral has converged and the duration measurements are complete, that is, the analysis need only be applied from just before the P arrival time to shortly after the source duration time beyond the P time. Thus it is likely in practice that the M_{ED} and Θ results will be stable and available within as little as 15 min after OT, a few minutes after the event has been

located with teleseismic observations.

It is also likely that the energy-duration methodology can be applied at local and regional distances when high dynamic-range, high sample-rate data is available. The main difficulty for $GCD < 30^\circ$ is that significant S signal may remain on the 1 Hz, high-frequency records, which complicates the determination of the P -wave duration for larger events. In this case, the direct P -wave radiation can often be isolated by applying the narrow-band, Gaussian filtering at higher frequencies. Additionally, at local and regional distances, the F^{SP} factor and attenuation relation will be different from those we used above to estimate radiated seismic energy (*i.e.*, Eq. 4).

Conclusions

We have presented an energy-duration procedure for rapid, robust and accurate determination of earthquake size and tsunamigenic potential, summarized through a moment magnitude, M_{ED} , and an energy-to-moment ratio, Θ .

An examination of the recent 26 December 2004, M9 Sumatra-Andaman and 17 July 2006, $M_w=7.7$ Java earthquakes illustrates the need for rapid, robust and accurate information about earthquake sizes and tsunamigenic potential, and shows the potential for our energy-duration procedure to help fill this need. Recall that we did not include these two events in our regression of M_0^{ED} against M_0^{CMT} , thus the following analysis is representative of the performance of the energy-duration methodology for future major and great earthquakes.

For the 2004 Sumatra-Andaman event, bulletins from the Pacific Tsunami Warning Center (PTWC) show that the event magnitude was evaluated at $M_{wp}=8.0$ at 15 minutes after OT, and at $M_m=8.5$ at 1 hour after OT (PTWC, 2004ab). The final CMT magnitude, available about 3 hours after OT, was $M_w^{CMT} = 9.0$, and, several months after the event, a moment magnitude of $M_w=9.1-9.3$ was derived from analysis of the Earth's normal modes (*e.g.*, Stein and Okal, 2005; Park, *et al.*, 2005). The energy-duration magnitude found in this study for this event is $M_{ED}=9.2$ (or $M_{ED}=9.1$ using average material properties at the source), a measure which is potentially available within about 20 minutes after OT. We determine an energy-to-moment ratio parameter $\Theta = -5.7$, a border-line value which would indicate, since this event is an interplate thrust, that it may be a tsunami earthquake. Later study of this event indicates that it was partially a tsunami earthquake (*e.g.*, Seno and Hirata, 2006; Kanamori, 2006), justifying a border-line value for Θ . In any case, given the size and tectonic setting of the event, the high probability that it would generate a major tsunami would be and was recognized rapidly.

For the 2006, Java event, bulletins from the Pacific Tsunami Warning Center (PTWC) show that the event magnitude was evaluated at $M_{wp}=7.2$ at 17 minutes after OT, and still at $M=7.2$ at about 3 hours after OT when sea-level gauge data indicate that a tsunami was generated (PTWC 2006ab). The final CMT magnitude, available about 1 hour after OT, was $M_w^{CMT}=7.7$, and the CMT message noted that this event had characteristics of a tsunami earthquake. The energy-duration magnitude found in this study for this event, potentially available within 20 minutes after OT, is $M_{ED}=7.8$ (or $M_{ED}=7.9$ using average material properties at the source). We determine an energy-to-moment ratio parameter $\Theta = -6.0$, a very low value indicating that, since the event is a shallow, interplate thrust, it has the characteristics of a tsunami earthquake, which is confirmed by later studies (*e.g.* Ammon *et al.*, 2006).

In summary, we have shown that our energy-duration procedure performs well for teleseismic observations at 30° to 90° GCD, producing magnitude estimates M_{ED} that match closely the M_w^{CMT} values for major and great earthquakes ($M_w^{CMT} \geq 7.0$), and energy-to-moment ratios Θ that agree with previous results and with the tsunamigenic character of the studied events. The energy-duration methodology may be applicable to smaller events and at regional and local distances ($GCD < \sim 30^\circ$).

Acknowledgements

We are grateful to Jack Boatwright and Dave Wald for their thorough and helpful reviews which greatly improved this manuscript. We also benefited from discussions with George Choy and Barry Hirshorn. The work of AL was supported by personal funds. AM and AP were supported in part through the 2005-07 Italian Civil Defense project S4. We use the Java program SeisGram2K (<http://www.alomax.net/software>) for seismogram analysis, processing and figures. The IRIS DMC (<http://www.iris.edu>) provided access to waveforms used in this study.

References

- Ammon, C. J., C. Ji, H.-K. Thio, D. Robinson, S. Ni, H. Kanamori, T. Lay, S. Das, D. Helmberger, V. Hjorleifsdottir, G. Ichinose, J. Polet, D. Wald, 2005. Rupture process of the 2004 Sumatra-Andaman earthquake, *Science*, **308**, 1133-1139.
- Ammon, C. J., H. Kanamori, T. Lay, and A. A. Velasco, 2006. The 17 July 2006 Java tsunami earthquake, *Geophys. Res. Lett.*, **33**, L24308, doi:10.1029/2006GL028005.
- Boatwright, J., and G. L. Choy, 1986. Teleseismic estimates of the energy radiated by shallow earthquakes, *J. Geophys. Res.* **91**, 2095–2112.
- Boatwright, J., G.L. Choy and L.C. Seekins, 2002. Regional Estimates of Radiated Seismic Energy, *Bull. Seism. Soc. Am.*, **92**, 1241–1255.
- Choy, G.L. and J.L. Boatwright, 1995. Global patterns of radiated seismic energy and apparent stress, *J. Geophys. Res.*, **100**, 18205-18228.
- Cocco, M., and J. Boatwright, 1993. The envelopes of acceleration time histories, *J. Geophys. Res.*, **83**, 1095-1114.
- Dziewonski, A.M. and D.L. Anderson, 1981. Preliminary Reference Earth Model (PREM), *Phys. Earth Planet. Inter.* **25**, 297-356.
- Dziewonski, A., T.A. Chou, and J. H. Woodhouse (1981. Determination of earthquake source parameters from waveform data for studies of global and regional seismicity, *J. Geophys. Res.*, **86**, 2825-2852.
- Ekström, G., 1994. Rapid earthquake analysis utilizes the internet: *Computers in Physics*, **8**, 632-638.
- Geist, E.L. , S.L. Bilek, D. Arcas, and V.V. Titov, 2006. Differences in tsunami generation between the December 26, 2004 and March 28, 2005 Sumatra earthquakes, *Earth Planets Space*, **58**, 185–193.
- Gusev, A. A., and V. M. Pavlov, 1991. Deconvolution of squared velocity waveform as applied to study of a noncoherent short-period radiator in the earthquake source, *Pure Appl. Geophys.* **136**, 235–244.
- Gutenberg, B., 1945. Amplitudes of P, PP, and S and magnitude of shallow earthquakes, *Bull. Seism. Soc. Am.*, **35**, 57 - 69.
- Hanks T.C. and H. Kanamori, 1979. A moment magnitude scale, *J. Geophys. Res.*, **84** (B5): 2348-2350.
- Haskell, N. A., 1964. Total energy and energy spectral density of elastic wave radiation from propagating faults, *Bull. Seism. Soc. Am.*, **54**, 1811-1841.
- Heinrich, P., A. Piatanesi and H. Hebert, 2001. Numerical modelling of tsunami generation and propagation from submarine slumps the 1998 Papua New Guinea event, *Geophys. J. Int.*, **145**, 97-111.
- Hirshorn, B., 2006. R.H. Hagemeyer Pacific Tsunami Warning Center, presentation for PTWS-WG1, Intergovernmental Coordination Group for the Pacific Tsunami Warning and Mitigation System (ICG/PTWS), Melbourne, Australia. (<http://ioc3.unesco.org/ptws>)

- Kanamori, H., 1972. Mechanism of Tsunami earthquakes, *Phys. Earth Planet. Int.*, **6**, 346-359.
- Kanamori, H., 1977. The energy release in great Earthquakes, *J. Geophys. Res.*, **82**, 2981-2987.
- Kanamori, H., 1978. Quantification of earthquakes, *Nature*, **271**, 411-414.
- Kanamori, H., 2006. The radiated energy of the 2004 Sumatra-Andaman earthquake, *AGU Chapman Volume*, v. XX, (in press).
- Kanamori, H. and M. Kikuchi, 1993. The 1992 Nicaragua earthquake; a slow tsunami earthquake associated with subducted sediments, *Nature*, **361**, 714-716, 1993.
- Kanjo, K., T. Furudate, and S. Tsuboi, 2006. Application of Mwp to the Great December 26, 2004 Sumatra Earthquake, *Earth Planets Space*, **58**, 121-126.
- Kawakatsu, H., 1995. Automated near-realtime CMT inversion, *Geophys. Res. Lett.*, **22**, 2569-2572.
- Kennett, B.L.N., E.R. Engdahl, and Buland R., 1995. Constraints on seismic velocities in the Earth from travel times, *Geophys. J. Int.*, **122**, 108-124
- Kerr, R. A., 2005. Failure to gauge the quake crippled the warning effort, *Science*, **307**, 201.
- Kikuchi, M., Y. Yamanaka, K. Abe, and Y. Morita, 1999. Source rupture process of the Papua New Guinea earthquake of July 17, 1998 inferred from teleseismic body waves, *Earth Planets Space*, **51**, 1319-1324.
- Lay, T., 2002. The Earth's Interior, in *International Handbook of Earthquake and Engineering Seismology*, (eds. W. H. K. Lee, H. Kanamori, P. C. Jennings, and C. Kisslinger), Academic Press, pp.829-860.
- Lay, T., H. Kanamori, C. J. Ammon, M. Nettles, S. N. Ward, R. C. Aster, S. L. Beck, S. L. Bilek, M. R. Brudzinski, R. Butler, H. R. DeShon, G. Ekström, K. Satake, and S. A. Sipkin, 2005. The great Sumatra-Andaman earthquake of 26 December 2004, *Science*, **308**, 1127-1133.
- Lomax, A., 2005. Rapid estimation of rupture extent for large earthquakes: application to the 2004, M9 Sumatra-Andaman mega-thrust, *Geophys. Res. Lett.*, **32**, L10314, doi:10.1029/2005GL022437.
- Lomax, A. and A. Michelini, 2005. Rapid Determination of Earthquake Size for Hazard Warning, *Eos Trans. AGU*, **86**, 19, 185-189.
- Menke, W., V. Levin, A Strategy to Rapidly Determine the Magnitude of Great Earthquakes, *Eos Trans. AGU*, **85**, 185, 10.1029/2005EO190002, 2005.
- NEIC, 2004. *NEIC Fast Moment Tensors*, in hypertext, http://neic.usgs.gov/neis/FM/fast_moment.html
- Newman, A.V., and E.A. Okal, 1998. Teleseismic Estimates of Radiated Seismic Energy: The E/M_0 Discriminant for Tsunami Earthquakes, *J. Geophys. Res.*, **103** (11), 26,885-98.
- NGDC, 2006. ETOPO2v2, 2-minute Gridded Global Relief Data, U.S. Department of Commerce, National Oceanic and Atmospheric Administration, National Geophysical Data Center.
- Okal, E.A., 2003. T Waves from the 1998 Papua New Guinea Earthquake and its Aftershocks: Timing the Tsunamigenic Slump, *Pure App. Geophys.*, **160**, 1843-1863.
- Okal, E. A., and J. Talandier, 1989. Mm: a variable period mantle magnitude, *J. Geophys. Res.* **94**, 4169-4193.
- Park, J., *et al.*, 2005. Earth's free oscillations excited by the 26 December 2004 Sumatra-Andaman earthquake, *Science*, **308**, 1139-1144.
- Pelayo, A.M. and D.A. Wiens, 1992. Tsunami earthquakes: slow thrust-faulting events in the accretionary wedge, *J. Geophys. Res.*, **97**, 15321-15337.
- Polet, J., H. Kanamori, 2000. Shallow subduction zone earthquakes and their tsunamigenic potential, *Geophys. J. Int.*, **142**, 684-782.

- PTWC, 2004a. Tsunami Bulletin Number 001, Issued at 0114Z 26 Dec 2004, *Pacific Tsunami Warning Center/NOAA/NWS*.
- PTWC, 2004b. Tsunami Bulletin Number 002, Issued at 0204Z 26 Dec 2004, *Pacific Tsunami Warning Center/NOAA/NWS*.
- PTWC, 2006a. Tsunami Bulletin Number 001, Issued at 0836Z 17 Jul 2006, *Pacific Tsunami Warning Center/NOAA/NWS*.
- PTWC, 2006b. Tsunami Bulletin Number 002, Issued at 1108Z 17 Jul 2006, *Pacific Tsunami Warning Center/NOAA/NWS*.
- Satake, K., 2002. Tsunamis, in *International Handbook of Earthquake and Engineering Seismology*, (eds. W. H. K. Lee, H. Kanamori, P. C. Jennings, and C. Kisslinger), Academic Press, pp.437-451.
- Seno, T. and K. Hirata, 2006. Did the 2004 Sumatra-Andaman Earthquake Involve a Component of Tsunami Earthquakes?, *Bull. Seism. Soc. Am.*, **97**, S296–S306.
- Shearer, P., 1999. *Introduction to Seismology*, 260 pp, Cambridge Univ. Press, New York.
- Stein, S., and E. A. Okal, 2005. Speed and size of the Sumatra earthquake, *Nature*, **434**, 581-582.
- Tsuboi, S., 2000. Application of M_{wp} to tsunami earthquake, *Geophys. Res. Lett.*, **27**, 3105–3108.
- Tsuboi, S., K. Abe, K. Takano, and Y. Yamanaka, 1995. Rapid determination of M_w from broadband P waveforms, *Bull. Seism. Soc. Am.*, **85**, 606-613.
- Tsuboi, S., P. M. Whitmore, and T. J. Sokolowski, 1999. Application of M_{wp} to deep and teleseismic earthquakes, *Bull. Seism. Soc. Am.*, **89**, 1345-1351.
- UNESCO, 2005. International Coordination Meeting for the Development of a Tsunami Warning and Mitigation System for the Indian Ocean within a Global Framework, *IOC Workshop Report 196*, 103 pp.
- Utsu, T., 2002. Relationships between magnitude scales, in *International Handbook of Earthquake and Engineering Seismology*, (eds. W. H. K. Lee, H. Kanamori, P. C. Jennings, and C. Kisslinger), Academic Press, pp.733-746.
- Vassiliou, M. S., and H. Kanamori, 1982. The energy release in earthquakes, *Bull. Seism. Soc. Am.*, **72**, 371–387.
- Venkataraman, A., and H. Kanamori, 2004. Observational constraints on the fracture energy of subduction zone earthquakes: *J. Geophys. Res.*, **109** (B5), B05302, 05310.01029/02003JB002549.
- Weinstein, S.A., and E.A. Okal, 2005. The mantle wave magnitude M_m and the slowness parameter θ : Five years of real-time use in the context of tsunami warning, *Bull. Seism. Soc. Am.*, **95**, 779-799.
- Weinstein, S., C. McCreery, B. Hirshorn, P. Whitmore, 2005. Comment on "A Strategy to Rapidly Determine the Magnitude of Great Earthquakes" by W. Menke and V. Levin, *Eos Trans. AGU*, **86**, 263, DOI: 10.1029/2005EO280005.
- Zeng, Y., K. Aki, and T.-L. Teng, 1993. Mapping of the high-frequency source radiation for the Loma Prieta earthquake, California, *J. Geophys. Res.*, **98**, 11,981-11,993.

Anthony Lomax

ALomax Scientific, Mouans-Sartoux, France; anthony@alomax.net, www.alomax.net

Alberto Michellini, Alessio Piatanesi

Istituto Nazionale di Geofisica e Vulcanologia (INGV), Via di Vigna Murata, 605, 00143 Roma, Italy;
www.ingv.it

Figure Captions

Figure 1

World map showing earthquakes used in study (*c.f.* Table 1). Symbols show earthquake type: Squares - interplate thrust; Diamonds - tsunami earthquake; Inverted triangles - intraplate; Triangles - downdip and deep; Circles - crustal and hybrid. Base map from NGDC (2006).

Figure 2

Processing steps for estimating the radiated seismic energy E for the 17 July 2006, M7.7 Java earthquake at station MN:IDI at 89° GCD to the northwest of the event. Upper trace: instrument corrected ground velocity seismogram; Lower: seismogram cut from 10 seconds before the P arrival to 10 seconds before the S arrival and integrated using Eq. 5. P and S indicate the ak135 predicted arrival times for the first P and S waves from the hypocentre.

Figure 3

Estimated radiated energy, E , from this study compared to E_S determined by the NEIC (Table 1). Events are labeled by their source types (see Table 1). The plotted energies, E , from this study for strike-slip events are not corrected for the strike-slip energy underestimate at teleseismic distances.

Figure 4

High-frequency (1-Hz Gaussian-filtered), vertical-component seismograms for the 26 December 2004, Sumatra-Andaman M9 mainshock at 00:58 UT (upper) and an M7.2 aftershock at 04:21 UT (lower) recorded at stations: MN:VTS in Bulgaria at about 70° GCD to the northwest of the events. Arrival times in the ak135 model (Kennett, Engdahl and Buland, 1995) are indicated for several major phases. Note on the M7.2 aftershock there is little or no high-frequency signal from later phases (e.g., PcP , PP , S) relative to the amplitude of the initial, direct P signal.

Figure 5

Estimation of the source duration T_0 for the 17 July 2006, M7.7 earthquake. a) Processing steps for estimating T_0 at station II:PALK at 31° GCD to the northwest of the event. Trace (0): raw, velocity seismogram; Trace (1): 1 Hz Gaussian filtered seismogram; Trace (2): velocity-squared time-series; Trace (3): smoothed velocity-squared envelope; Trace (4): stacked, smoothed, velocity-squared envelopes from all stations for this event. b) Top: stacked, smoothed, velocity-squared envelopes from all stations; Other traces: smoothed, velocity-squared envelopes from several stations for this event. P and S indicate the ak135 predicted arrival times for the first P and S waves from the hypocentre. 5 and 3 indicates the estimated source P_{end} times at envelope levels of 50% and 33% of the peak value, respectively; the mean of these two values on the station stack gives $T_0 = 157$ sec for this event.

Figure 6

Energy-duration magnitude M_{ED} from this study compared to CMT magnitude M_w^{CMT} . The lower (upper) bounds on M_{ED} obtained using $E - \sigma_E$ and 50%-peak duration ($E + \sigma_E$ and 33%-peak duration) are indicated by grey triangles.

Figure 7

Estimated radiated energy E compared to the moment M_0^{ED} from this study. Lines of constant Θ are

shown for $\Theta = -4.9$, the expected value for all earthquakes, and $\Theta = -5.5$, below which indicates a possible tsunami earthquake. Events are labelled by their source types (see Table 1).

Figure 8

Broadband, moment magnitude M_{wp} from this study compared to CMT magnitude M_w^{CMT} . Events are labeled by their source types (see Table 1).

Table 1

Events used in this study and energy-duration results

| Origin time | Event | Type* | NEIC | | | | CMT | | | | this study, energy-duration results | | | | | | |
|------------------|------------------|-------|-----------------|------------------|---------------|----------------|---------------|----------------------|-------------|------------------------|-------------------------------------|--------------|---------------------------------|---------------------|----------|----------|----------|
| | | | latitude (°) | longitude (°) | depth (km) | E_s (N-m) | depth (km) | M_0^{CMT} (N-m) | M_w^{CMT} | T_0^\dagger (sec) | T_0 (sec) | E (N-m) | \bar{E} corrected (N-m) | M_0^{ED} (N-m) | M_{ED} | Θ | M_{wp} |
| 1992.09.02 00:15 | Nicaragua | T | 11.74 | -87.34 | 44 | 2.6E+14 | 15 | 3.4E+20 | 7.6 | 37 | 175 | 1.9E+14 | 1.9E+14 | 4.4E+20 | 7.7 | -6.4 | 7.3 |
| 1992.12.12 05:29 | Flores Indonesia | I | -8.48 | 121.90 | 49 | 6.6E+15 | 20 | 5.1E+20 | 7.8 | 36 | 91 | 7.8E+15 | 7.8E+15 | 1.1E+21 | 8.0 | -5.1 | 7.7 |
| 1993.07.12 13:17 | Hokkaido | I | 42.85 | 139.20 | 18 | 8.7E+15 | 17 | 4.7E+20 | 7.7 | 33 | 78 | 1.0E+16 | 1.0E+16 | 9.8E+20 | 7.9 | -5.0 | 7.6 |
| 1994.01.17 12:30 | S California | R | 34.21 | -118.54 | 21 | 1.1E+14 | 17 | 1.2E+19 | 6.7 | 11 | 17 | 1.2E+14 | 1.2E+14 | 8.9E+18 | 6.6 | -4.9 | 6.9 |
| 1994.06.02 18:17 | Java | T | -10.48 | 112.84 | 6 | 1.2E+14 | 15 | 5.3E+20 | 7.7 | 23 | 97 | 3.8E+14 | 3.8E+14 | 2.6E+20 | 7.5 | -5.8 | 7.5 |
| 1994.06.09 00:33 | Bolivia | D | -13.84 | -67.55 | 631 | 3.2E+16 | 647 | 2.6E+21 | 8.2 | 40 | 42 | 4.8E+16 | 4.8E+16 | 3.0E+21 | 8.2 | -4.8 | 7.8 |
| 1994.10.04 13:23 | Kuril | P | 43.77 | 147.32 | 61 | 1.1E+17 | 68 | 3.0E+21 | 8.3 | 50 | 67 | 6.4E+16 | 6.4E+16 | 3.3E+21 | 8.3 | -4.7 | 7.8 |
| 1995.12.03 18:01 | Kuril | I | 44.66 | 149.30 | 23 | 2.4E+15 | 26 | 8.2E+20 | 7.9 | 28 | 71 | 2.9E+15 | 2.9E+15 | 7.5E+20 | 7.9 | -5.4 | 7.6 |
| 1996.02.17 05:59 | Irian Jaya | I | -0.89 | 136.95 | 11 | 8.5E+15 | 15 | 2.4E+21 | 8.2 | 59 | 114 | 8.9E+15 | 8.9E+15 | 1.6E+21 | 8.1 | -5.3 | - |
| 1996.02.21 12:51 | Peru | T | -9.59 | -79.59 | 4 | - | 15 | 2.2E+20 | 7.5 | 21 | 75 | 2.2E+14 | 2.2E+14 | 1.4E+20 | 7.4 | -5.8 | 7.3 |
| 1998.07.17 08:49 | Papua New Guinea | I | -2.96 | 141.93 | 7 | 2.4E+14 | 15 | 3.7E+19 | 7.1 | 15 | 49 | 1.2E+14 | 1.2E+14 | 5.2E+19 | 7.1 | -5.6 | 6.9 |
| 1999.04.08 13:10 | Russia-China | D | 43.61 | 130.35 | 576 | 9.0E+14 | 575 | 5.1E+19 | 7.1 | 17 | 11 | 7.3E+14 | 7.3E+14 | 4.4E+19 | 7.0 | -4.8 | 7.0 |
| 1999.08.17 00:01 | Turkey | S | 40.75 | 29.86 | 13 | 8.1E+15 | 17 | 2.9E+20 | 7.6 | 41 | 51 | 1.2E+15 | 1.2E+16 | 4.6E+20 | 7.7 | -4.6 | 7.6 |
| 1999.09.20 17:47 | Taiwan | R | 23.77 | 120.98 | 8 | 1.5E+15 | 21 | 3.4E+20 | 7.6 | 40 | 58 | 2.7E+15 | 2.7E+15 | 2.6E+20 | 7.5 | -5.0 | 7.6 |
| 1999.10.16 09:46 | S California | S | 34.59 | -116.27 | 20 | 1.9E+15 | 15 | 6.0E+19 | 7.1 | 20 | 42 | 1.5E+14 | 1.5E+15 | 1.2E+20 | 7.3 | -4.9 | 7.4 |
| 2000.10.06 04:30 | W Honshu | S | 35.46 | 133.13 | 10 | 2.9E+15 | 15 | 1.2E+19 | 6.7 | 12 | 54 | 4.8E+13 | 4.8E+14 | 9.9E+19 | 7.3 | -5.3 | 6.8 |
| 2001.01.26 03:16 | S India | R | 23.42 | 70.23 | 10 | 6.4E+15 | 20 | 3.4E+20 | 7.6 | 48 | 33 | 7.6E+15 | 7.6E+15 | 1.9E+20 | 7.5 | -4.4 | 7.8 |
| 2001.02.28 18:54 | Washington | P | 47.15 | -122.73 | - | 1.1E+14 | 51 | 1.9E+19 | 6.8 | 12 | 15 | 1.1E+14 | 1.1E+14 | 1.4E+19 | 6.7 | -5.1 | 6.6 |
| 2001.03.24 06:27 | W Honshu | P | 34.08 | 132.53 | - | 5.5E+13 | 47 | 1.9E+19 | 6.8 | 12 | 34 | 7.4E+13 | 7.4E+13 | 4.1E+19 | 7.0 | -5.7 | 7.0 |
| 2001.06.23 20:33 | Peru | I | -16.27 | -73.64 | 8 | 2.9E+16 | 30 | 4.7E+21 | 8.4 | 86 | 135 | 1.5E+16 | 1.5E+16 | 4.5E+21 | 8.4 | -5.5 | 7.5 |
| 2002.11.03 22:12 | Alaska | RS | 63.52 | -147.44 | 4 | 3.3E+16 | 15 | 7.5E+20 | 7.9 | 47 | 39 | 2.8E+15 | 2.8E+16 | 4.6E+20 | 7.7 | -4.2 | 7.4 |
| 2003.05.21 18:44 | N Algeria | R | 36.96 | 3.63 | 9 | 3.4E+14 | 15 | 2.0E+19 | 6.8 | 12 | 28 | 2.2E+14 | 2.2E+14 | 2.5E+19 | 6.9 | -5.1 | 7.0 |
| 2003.09.25 19:50 | Hokkaido | I | 41.82 | 143.91 | 13 | 2.2E+16 | 28 | 3.1E+21 | 8.3 | 67 | 74 | 1.4E+16 | 1.4E+16 | 1.8E+21 | 8.1 | -5.1 | 7.9 |
| 2003.09.27 11:33 | Siberia | S | 50.04 | 87.81 | 1 | 5.1E+15 | 15 | 9.4E+19 | 7.2 | 12 | 68 | 5.7E+14 | 5.7E+15 | 4.8E+20 | 7.7 | -4.9 | 7.4 |
| 2003.12.26 01:56 | S Iran | S | 29.00 | 58.31 | 10 | 6.1E+14 | 15 | 9.3E+18 | 6.6 | 10 | 31 | 3.2E+13 | 3.2E+14 | 3.5E+19 | 7.0 | -5.0 | 6.7 |
| 2004.12.23 14:59 | Macquarie | S | -50.15 | 160.37 | - | 5.2E+16 | 28 | 1.6E+21 | 8.1 | 53 | 59 | 8.3E+15 | 8.3E+16 | 3.1E+21 | 8.3 | -4.6 | 7.8 |
| 2004.12.26 00:58 | Sumatra-Andaman | IT? | 3.30 | 95.98 | 39 | 1.4E+17 | 29 | 4.0E+22 | 9.0 | 190 | 420 | 1.4E+17 | 1.4E+17 | 7.7E+22 | 9.2 | -5.7 | 8.1 |
| 2005.03.28 16:09 | N Sumatra | I | 2.09 | 97.11 | - | 6.7E+16 | 30 | 1.1E+22 | 8.6 | 99 | 94 | 5.0E+16 | 5.0E+16 | 4.8E+21 | 8.4 | -5.0 | 8.2 |
| 2005.06.13 22:44 | Chile | W | -19.99 | -69.20 | 115 | 5.4E+15 | 95 | 5.1E+20 | 7.7 | 36 | 53 | 1.6E+16 | 1.6E+16 | 1.1E+21 | 8.0 | -4.8 | 7.6 |
| 2005.07.24 15:42 | Nicobar | S | 7.92 | 92.19 | 16 | 1.2E+16 | 12 | 8.8E+19 | 7.2 | 25 | 39 | 8.4E+14 | 8.4E+15 | 2.5E+20 | 7.5 | -4.5 | 7.2 |
| 2005.08.16 02:46 | Honshu | I | 38.28 | 142.04 | 36 | 3.8E+14 | 37 | 7.4E+19 | 7.2 | 20 | 53 | 3.2E+14 | 3.2E+14 | 1.6E+20 | 7.4 | -5.7 | 7.4 |
| 2005.10.08 03:50 | Pakistan | R | 34.54 | 73.59 | 26 | 3.1E+15 | 12 | 2.9E+20 | 7.6 | 18 | 54 | 2.8E+15 | 2.8E+15 | 2.4E+20 | 7.5 | -4.9 | 7.6 |
| 2006.02.22 22:19 | Mozambique | N | -21.32 | 33.58 | 11 | 4.4E+14 | 12 | 4.5E+19 | 7.0 | 16 | 26 | 6.4E+14 | 6.4E+14 | 3.7E+19 | 7.0 | -4.8 | 7.3 |
| 2006.05.16 10:39 | Kermadec | D | 31.78 | 179.31 | 151 | - | 155 | 1.7E+20 | 7.4 | 25 | 25 | 5.6E+15 | 5.6E+15 | 2.2E+20 | 7.5 | -4.6 | 7.5 |
| 2006.07.17 08:19 | Indonesia | T | -9.25 | 107.41 | 34 | 3.2E+14 | 20 | 4.0E+20 | 7.7 | 100 | 157 | 6.6E+14 | 6.6E+14 | 7.1E+20 | 7.8 | -6.0 | 7.2 |

* Earthquake type: I - interplate thrust; T - tsunami earthquake; W - downdip; P - intraplate; D - deep; S - strike-slip crustal; R - reverse-faulting crustal; N - normal-faulting crustal.

† 2 x CMT half-duration

Figure 1

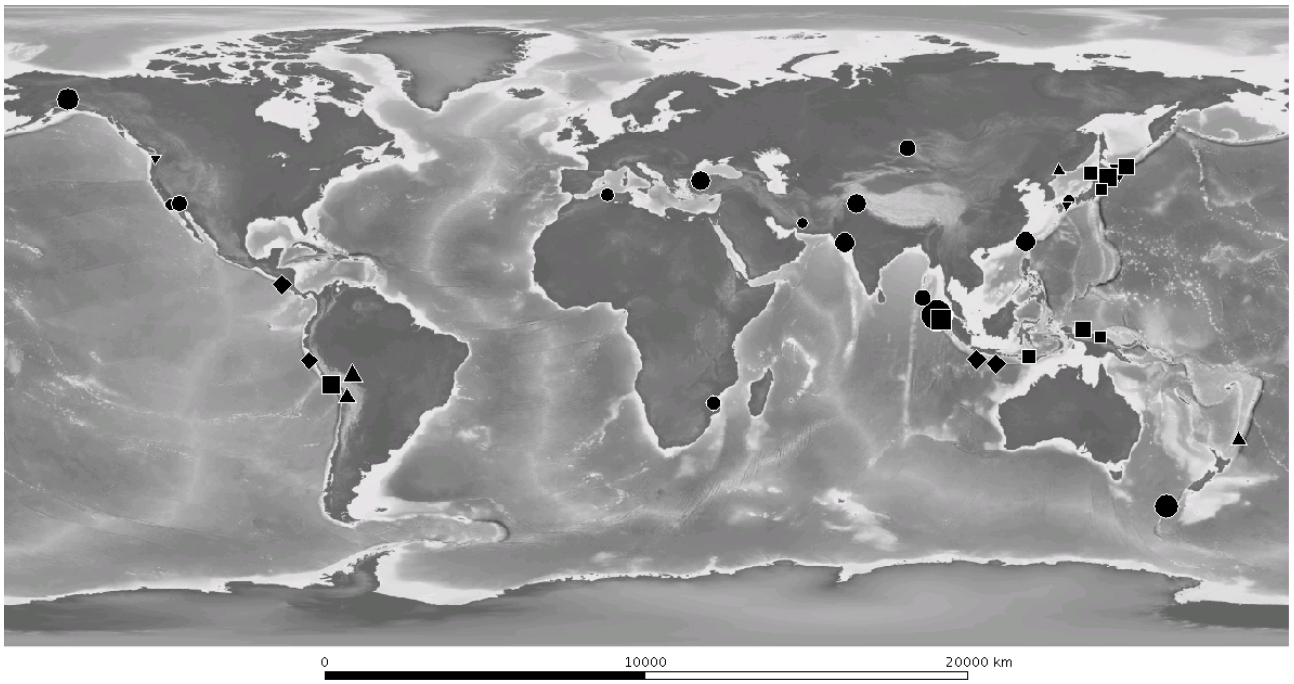


Figure 2

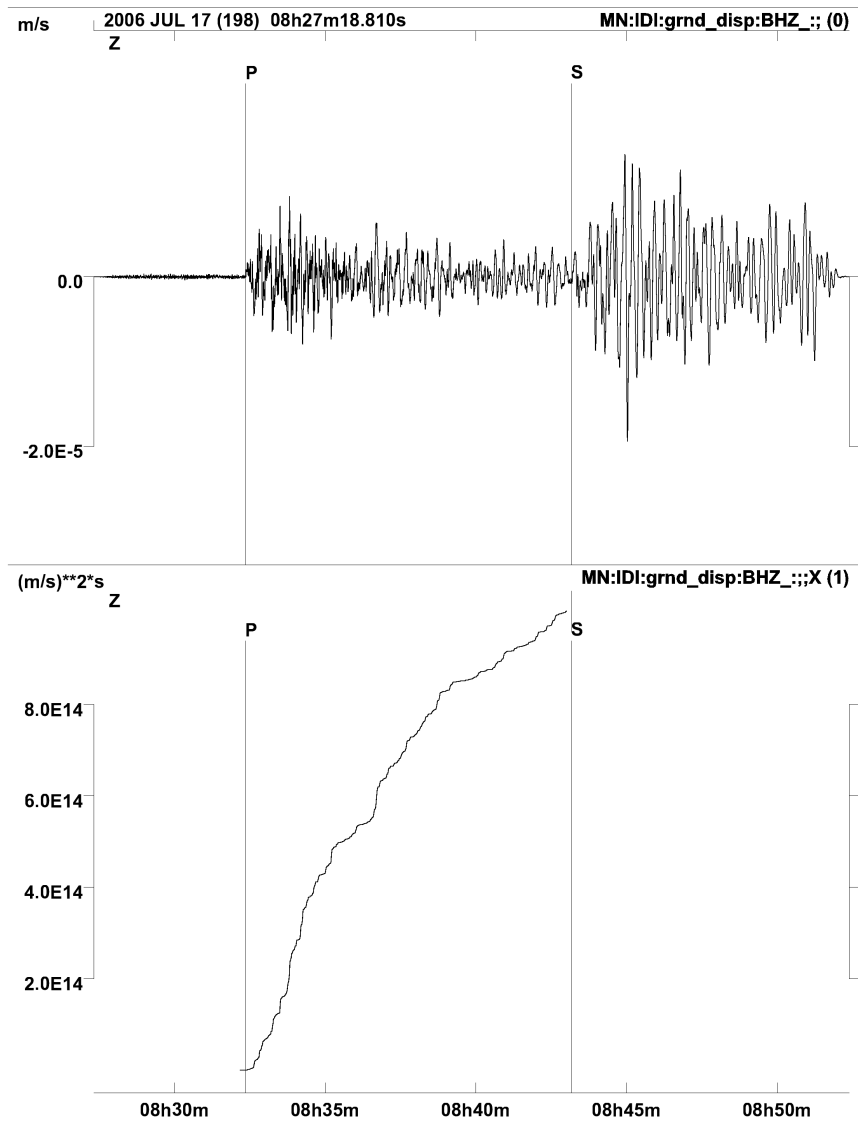


Figure 4

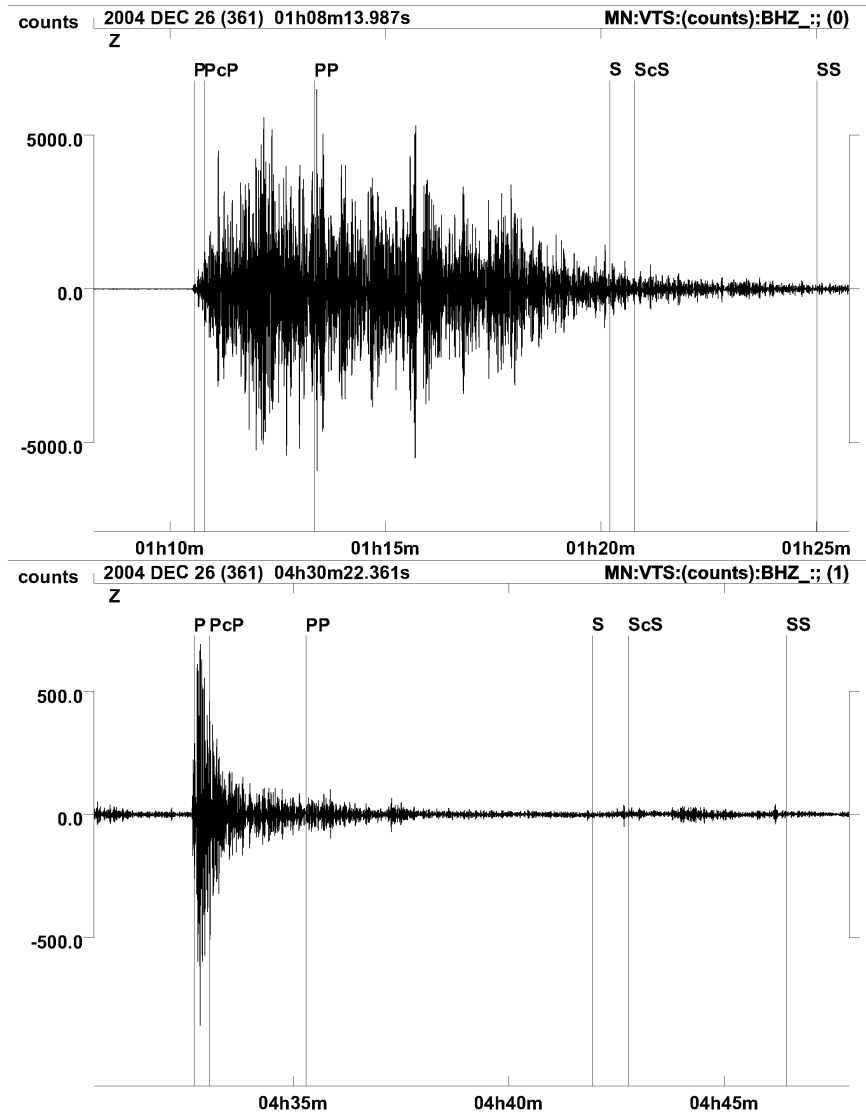


Figure 5a

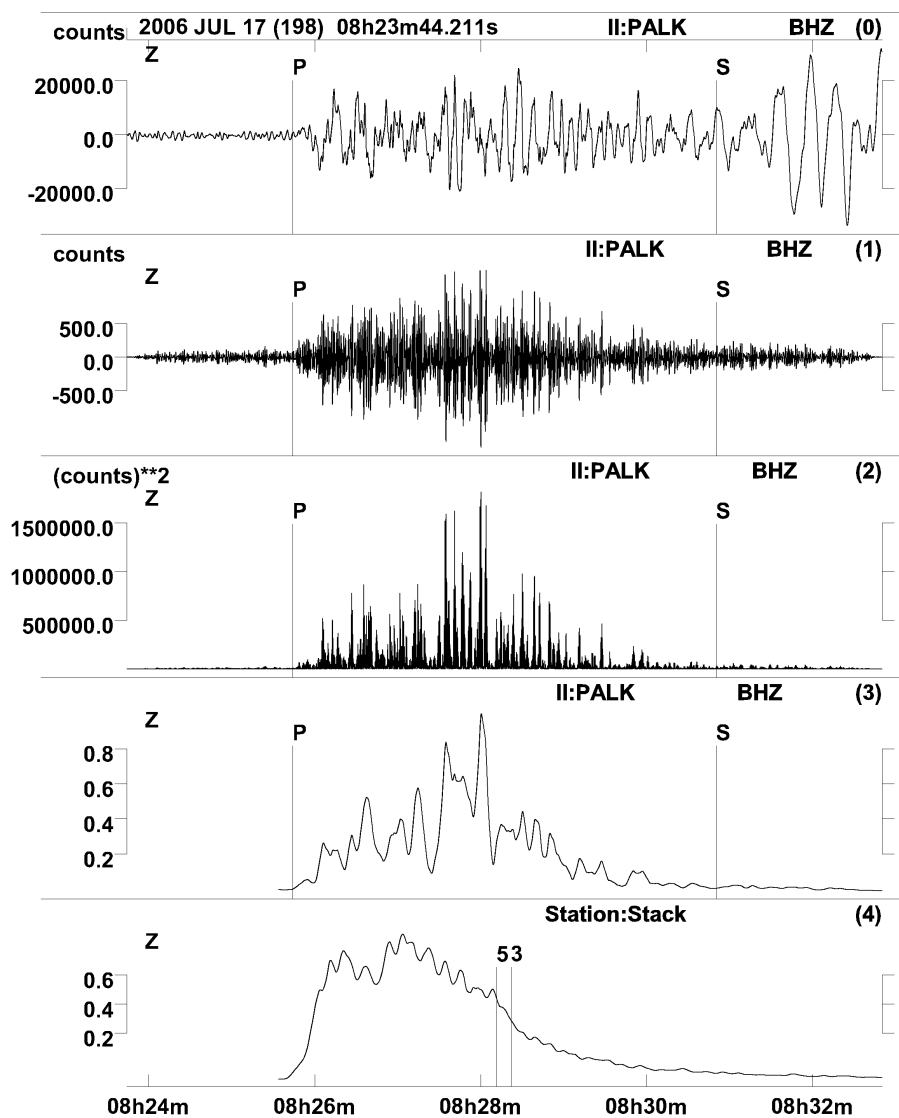


Figure 5b

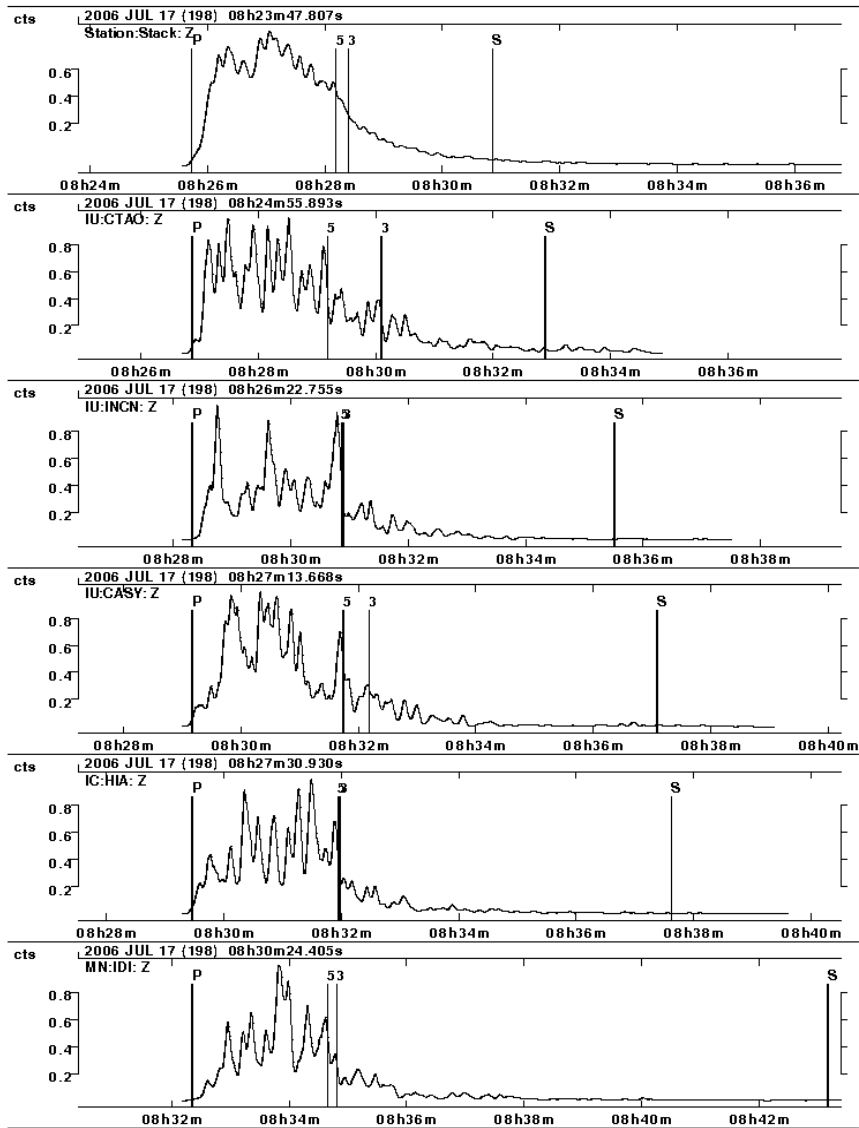


Figure 6

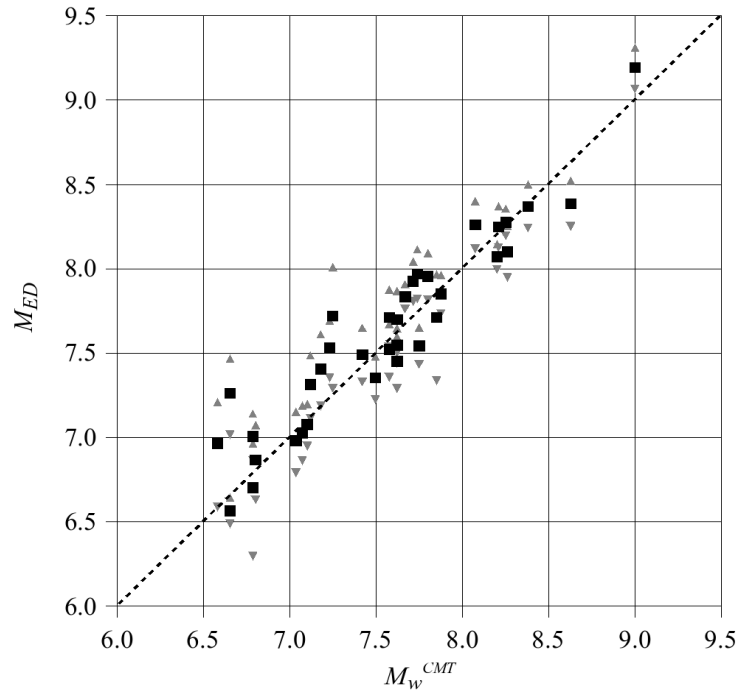


Figure 7

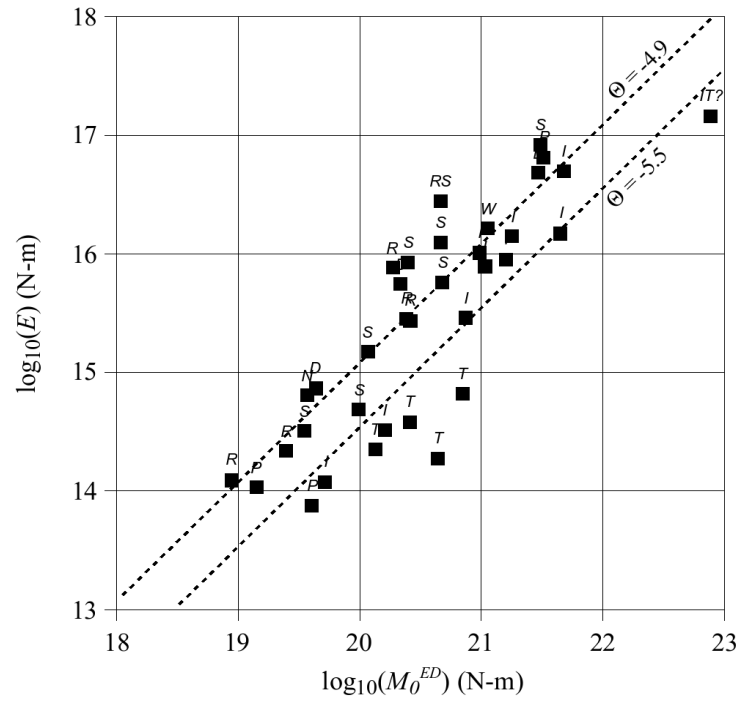


Figure 8

